

Supplementary Information for:

Engineering the electronic properties of single-layer covalent organic frameworks

Antonios Raptakis,^{†,§} Arezoo Dianat,[†] Alexander Croy,[‡] and Gianaurelio
Cuniberti^{*,†,¶}

[†]*Institute for Materials Science and Max Bergmann Center of Biomaterials, TU Dresden,
01062 Dresden, Germany*

[‡]*Institute of Physical Chemistry, Friedrich Schiller University Jena, 07737 Jena, Germany*

[¶]*Dresden Center for Computational Materials Science (DCMS), TU Dresden, 01062
Dresden, Germany*

[§]*Max Planck Institute for the Physics of Complex Systems, 01187 Dresden, Germany*

E-mail: gianaurelio.cuniberti@tu-dresden.de

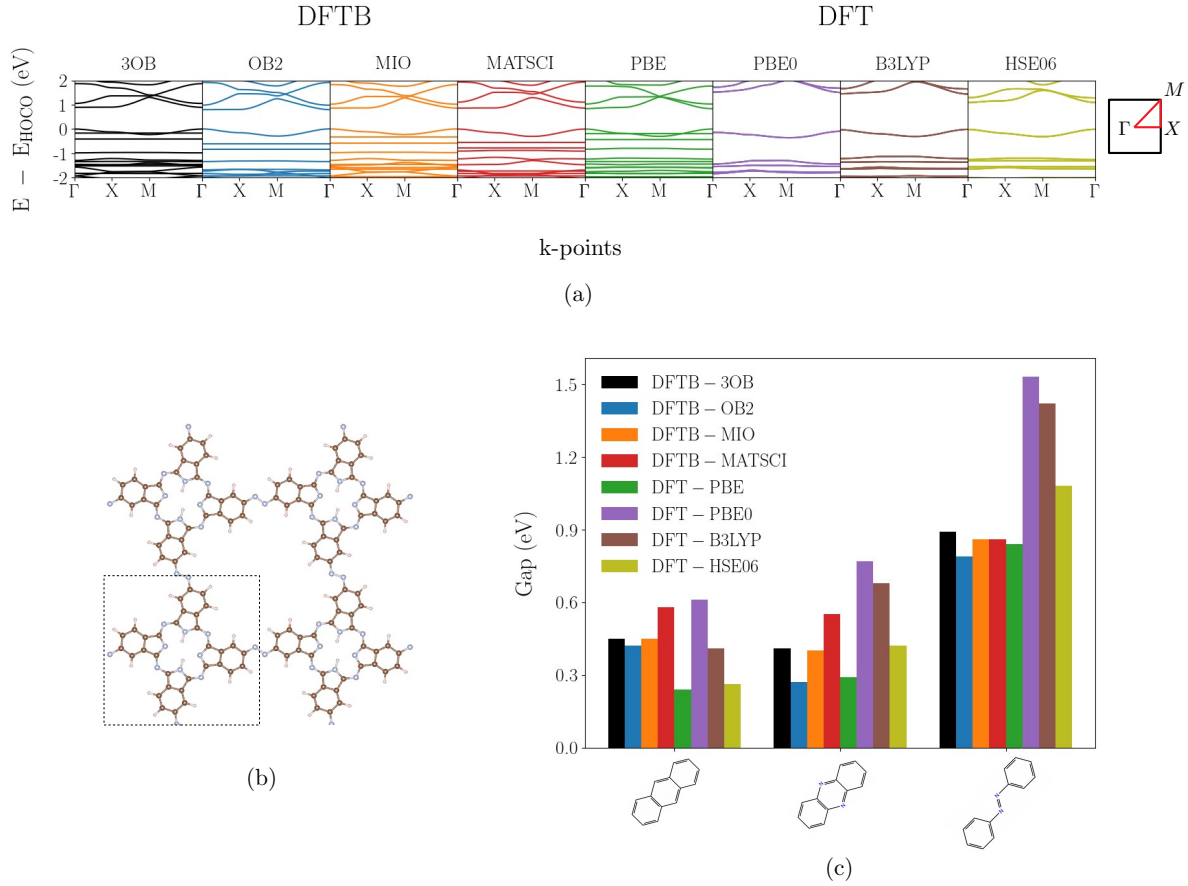


Figure S1: (a) Electronic band-structure for Phthal-Azo-COF comparing the different parametrizations of a semi-empirical method (DFTB) to the different potential of an *ab-initio* method (DFT). From the left to right, the first four concern DFTB and the rest DFT. On the top of each plot is labeled the particular reference to different parametrization or potential. (b) The structure of Phthal-Azo-COF. (c) Electronic gaps of the Phthal based COFs using different Slater Koster parametrizations for DFTB and xc-correlation potential for DFT for selected molecules: anthracene, phenazine, azo (from left to right).

Table S1: Electronic gap in eV for H2-Phthal based COFs with different linkages.

Linkage/Linker	3OB	OB2	MIO	MATSCI	PBE	PBE0	B3LYP	HSE06
Anthracene	0.45	0.42	0.45	0.58	0.24	0.61	0.41	0.26
Phenazine	0.41	0.27	0.4	0.55	0.29	0.77	0.68	0.42
Azo	0.89	0.79	0.86	0.86	0.84	1.53	1.42	1.08

The influence of the parametrization of the matrix elements on the electronic band structure is studied by using different Slater-Koster sets: 3ob-3-1 (3OB) and mio-1-1 (MIO), ob2-1-1 (OB2) and matsci-0-3 (MATSCI). In some selected cases, we have carried out benchmark calculations based on full DFT as implemented in the VASP package,¹ and using the

GGA-PBE level for the exchange-correlation functional.² The representation of the wavefunction was implemented through plane-waves using a cut-off energy of 500 eV. The number of k -points was the same as in the DFTB calculations.

As we scrutinize the effect of different Slater-Koster parametrizations, we did the same with hybrid functionals for DFT. Hybrid functionals are particularly implemented for electronic calculations and their parameters affect the resultant energy eigenvalues. To compare the electronic structure and band-gap to PBE, single point calculation of the optimized structure with PBE was done, activating the hybrid functionals PBE0,^{3,4} B3LYP^{5,6} and HSE06.^{7,8}

Figure S1(a) shows the calculated electronic band structures using different DFTB parametrizations and different DFT XC-functionals. The band-path at the k -space is obtained by high-symmetry points of the irreducible Brillouin zone for the square lattice topology. The first four graphs from left to right in Fig. S1(a) show the influence of different Slater-Koster parametrizations for Phthal-Azo-COF, whose structure is shown in Fig. S1(b). There are some overall shifts of the energy bands, but in all cases the gap is found at the Γ -point, which is consistent with the DFT-PBE calculation also shown in Fig. S1(a). This is to be expected, since all Slater-Koster parametrizations have been implemented by the best fits to PBE calculations.

Other XC-functionals than PBE yield, however, stronger modifications of the band structure. This is illustrated in the last three panels of Fig. S1(a). The PBE0 hybrid functional gives the largest band shifts, while HSE06 yields the smallest shifts when compared to the other two hybrid functionals (B3LYP and PBE0), being also closer to PBE. For all cases, the gap remains direct and the gap-point is found at the same high symmetry point (Γ -point) as for DFTB and DFT-PBE.

It is interesting to compare the results of the electronic band gap between DFTB and DFT for selected COF structures. This is shown in Fig. S1(c) and summarized in Table S1 for Phthal-Phenazine, -Anthracene and -Azo. For the linkers with fused rings (Anthracene

and Phenazine), MATSCI gives the highest (0.58 and 0.55 eV) and OB2 the lowest (0.42 and 0.27 eV) band gap. However, PBE yields the lowest electronic band-gap (0.24 and 0.29 eV), indicating a semi-metal instead of a semiconductor. As already mentioned, using different XC-functionals can shift the energy eigenvalues, and thus widen or shorten the electronic gap. There is a trend between the functionals, PBE0 gives a higher value and HSE06 a lower value while the values with B3LYP lie in between. These values are always higher than PBE, where PBE0 can give a gap even two times higher than PBE. For the Azo linkage, 3OB gives the higher value and OB2 the lower. All of the different parametrizations give close values to PBE. The trend among the hybrid functionals remains the same, and the tendency between hybrid functionals and PBE remains similar.

Table S2: The electronic band gap of the TBPor and Phthal based COFs using two different Slater Koster parametrizations, 3ob-3-1 (3OB) and matsci-0-3 (MATSCI). As PBP-0 and BDPE-0 are denoted the bridges that have no phenyl ring as linker in the bridge.

Linkage/Linker	H2-TBPor		H2-Phthal	
	3OB	MATSCI	3OB	MATSCI
Imine	1.20	1.26	0.98	0.97
Azo	1.04	0.87	0.86	0.65
BPH	1.26	1.15	1.00	0.85
BBH	1.55	1.60	1.3	1.27
Anthracene	0.60	0.81	0.45	0.62
Tetracene	0.42	0.67	0.34	0.57
Pentacene	0.31	0.51	0.25	0.44
Hexacene	0.22	0.38	0.14	0.32
Heptacene	0.14	0.28	0.08	0.22
Phenazine	0.50	0.66	0.41	0.55
QL-Ph	0.22	0.21	0.15	0.13
DQL-Ph	0.06	0.00	0.02	0.00
PBP-0	1.50	1.49	1.60	1.18
PBP-1	1.50	1.52	1.60	1.21
PBP-2	1.31	1.52	1.46	1.20
PBP-3	1.24	1.52	1.38	1.19
BDPE-0	-	1.65	-	1.33
BDPE	-	1.65	-	1.33
BDPE-2	-	1.65	-	1.33
BDPE-3	-	1.65	-	1.33
BDPE-4	-	1.65	-	1.33

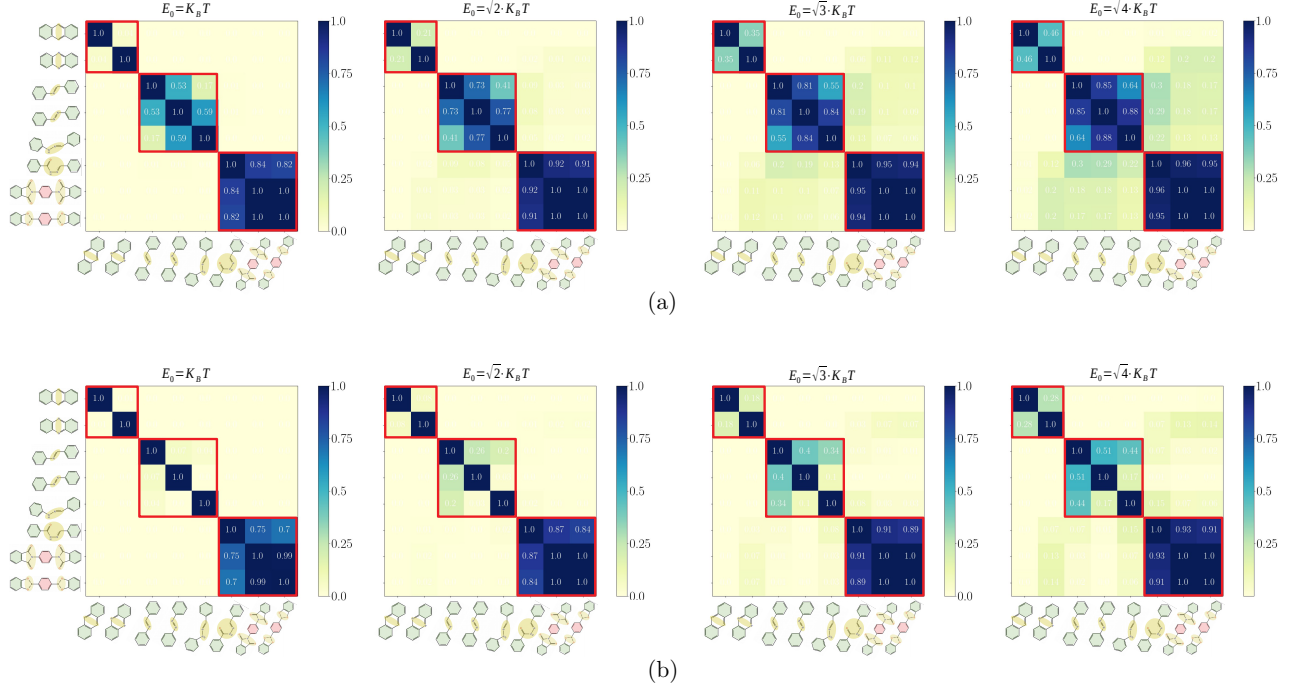


Figure S2: Similarity matrix for different values of the arbitrary constant E_0 for Phthal based COFs: (a) as given by Eq. 4, (b) in the metrics of Eq. 2 have been added the bands under the valence band and over the conduction band.

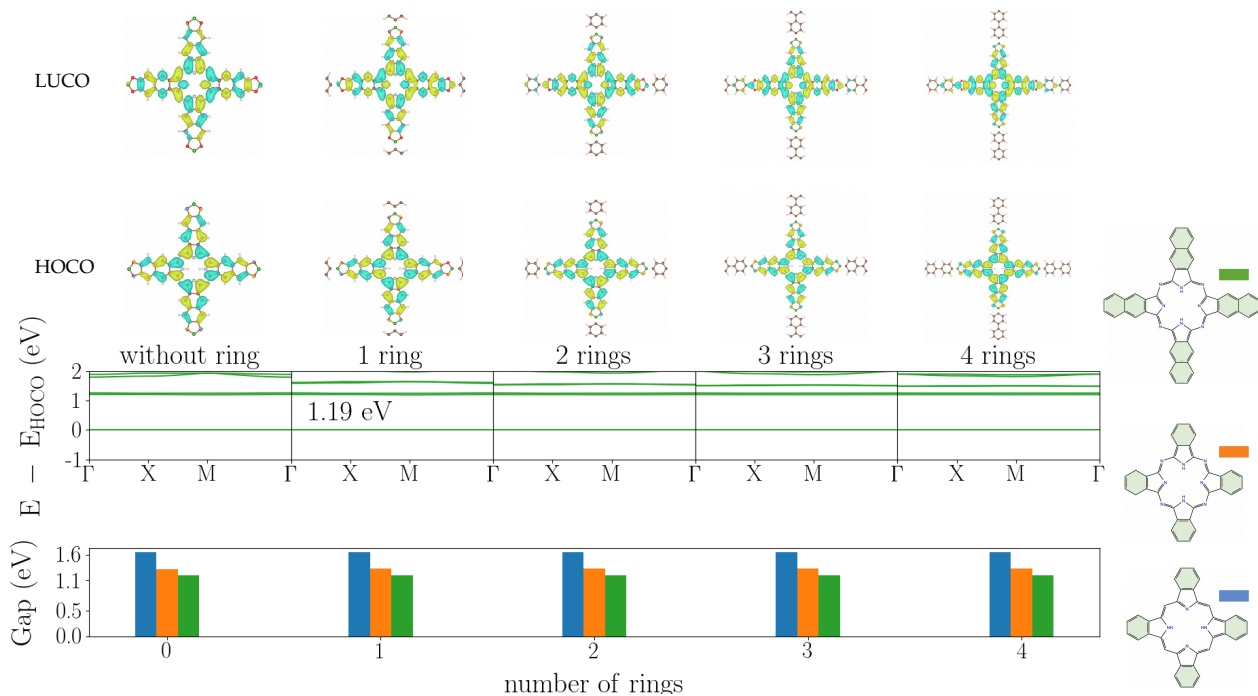


Figure S3: Extra fused rings between the core of Phthal (tetrad-Phthal) and the bridge BDPE. From the left to right the plots are referred to different number of rings in the bridge. Top: charge distribution of the HOCO and LUCO levels, middle: electronic band structure, bottom: bar-plots comparison of the electronic gap for the different cores, blue is referred to TBPor, orange to Phthal and green to tetrad-Phthal.

Table S3: The values of electronic gap and mass density for H2-Phthal based COFs while the mass density is increasing.

Linker	Gap(eV)
Ph-Ph	0.09
QL-Ph	1.02
QL-Ph +C	1.00
QL-Ph +ethene	1.02
QL-Ph +3C	1.02
An-DP	0.02
DQL-DPh	1.06
DQL-DPh +C	1.07
DQL-DPh +ethene	1.05
DQL-DPh +3C	1.07
DQL-DPh +4C	1.07
DQL-DPh +5C	1.07
DQL-DPh +6C	1.07

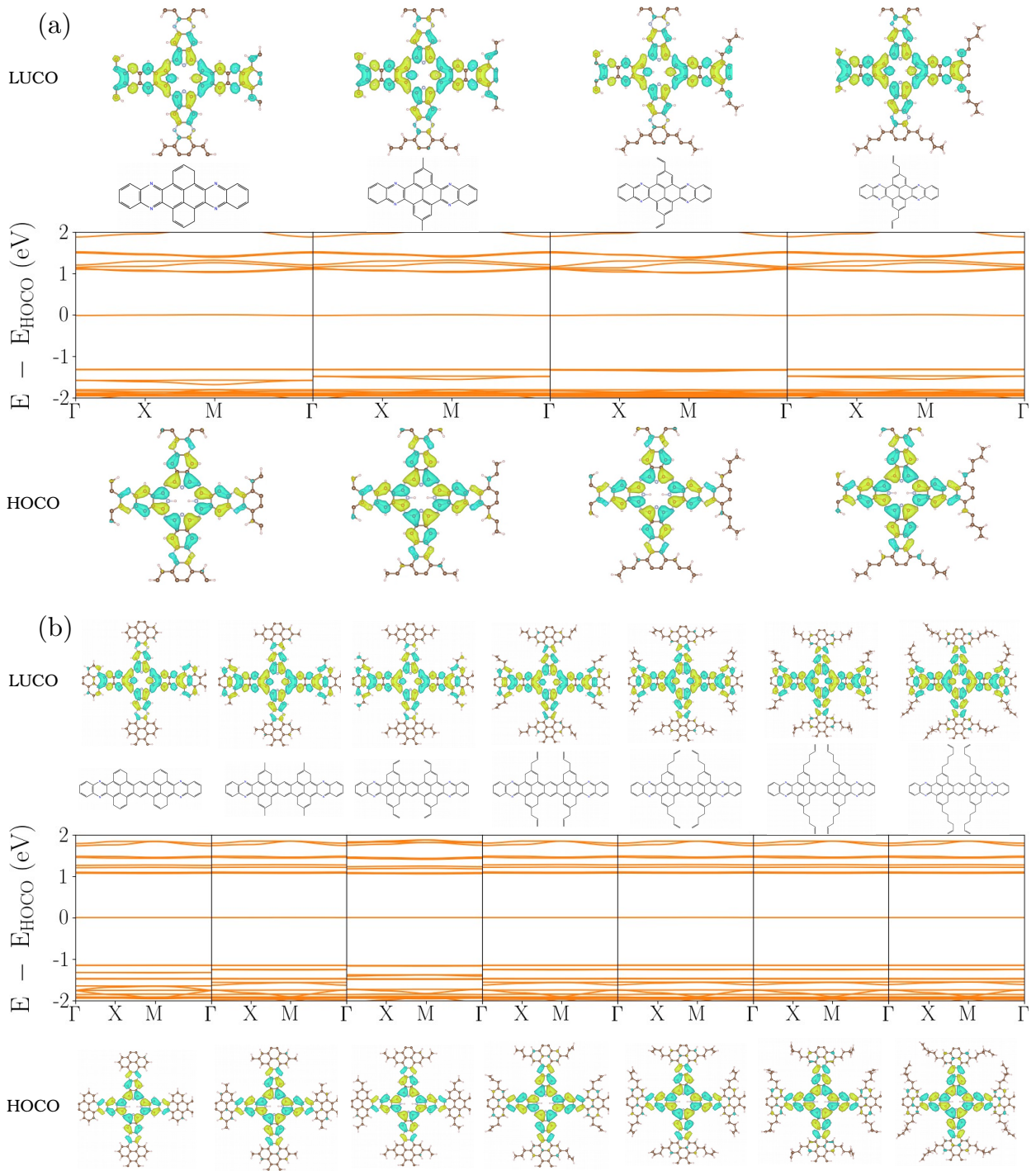


Figure S4: Electronic band structure for (a) Phthal-QL-PH-COF and (b) Phthal-DQL-DPH-COF after we add carbon atoms as an aside group connected with specific atoms on the linker. The corresponding charge distribution of the HOMO and LUMO band are on the top and bottom of the electronic band structure plots.

References

- (1) <https://www.vasp.at/>.
- (2) Perdew, J. P.; Burke, K.; Ernzerhof, M. Generalized gradient approximation made simple. *Physical Review Letters* **1996**, *77*, 3865–3868.
- (3) Perdew, J. P.; Ernzerhof, M.; Burke, K. Rationale for mixing exact exchange with density functional approximations. *Journal of Chemical Physics* **1996**, *105*, 9982–9985.
- (4) Adamo, C.; Barone, V. Toward reliable density functional methods without adjustable parameters: The PBE0 model. *Journal of Chemical Physics* **1999**, *110*, 6158–6170.
- (5) Stephens, P. J.; Devlin, F. J.; Chabalowski, C. F.; Frisch, M. J. Ab Initio calculation of vibrational absorption and circular dichroism spectra using density functional force fields. *Journal of Physical Chemistry* **1994**, *98*, 11623–11627.
- (6) Kim, K.; Jordan, K. D. Comparison of density functional and MP2 calculations on the water monomer and dimer. *Journal of Physical Chemistry* **1994**, *98*, 10089–10094.
- (7) Heyd, J.; Scuseria, G. E.; Ernzerhof, M. Hybrid functionals based on a screened Coulomb potential. *Journal of Chemical Physics* **2003**, *118*, 8207–8215.
- (8) Krukau, A. V.; Vydrov, O. A.; Izmaylov, A. F.; Scuseria, G. E. Influence of the exchange screening parameter on the performance of screened hybrid functionals. *Journal of Chemical Physics* **2006**, *125*, 224106.